The Journal of Immunology

A System for In Vitro Generation of Mature Murine Plasma Cells Uncovers Differential *Blimp-1*/*Prdm1* Promoter Usage

Emily Robinson, Matthew A. Care, Kieran Walker, Michelle Campbell, Reuben M. Tooze and Gina M. Doody

J Immunol 2022; 208:514-525; Prepublished online 15 December 2021;
doi: 10.4049/jimmunol.2100004
http://www.jimmunol.org/content/208/2/514

The Journal of Immunology is published twice each month by
The American Association of Immunologists, Inc.,
1451 Rockville Pike, Suite 650, Rockville, MD 20852

Print ISSN: 0022-1767 Online ISSN: 1550-6606.

A System for In Vitro Generation of Mature Murine Plasma Cells Uncovers Differential *Blimp-1*/*Prdm1* Promoter Usage

Emily Robinson,* Matthew A. Care,* Kieran Walker,* Michelle Campbell,* Reuben M. Tooze,*,† and Gina M. Doody*

Upon encounter with Ag, B cells undergo a sequential process of differentiation to become Ab-secreting plasma cells. Although the key drivers of differentiation have been identified, research has been limited by the lack of in vitro models recapitulating the full process for murine B cells. In this study, we describe methodology using BCR or TLR ligation to obtain plasma cells that are phenotypically mature, have exited cell cycle and express a gene signature concordant with long-lived plasma cells. Dependent on the initial stimuli, the transcriptomes also show variation including the enhanced expression of matrisome components after BCR stimulation, suggestive of unique functional properties for the resultant plasma cells. Moreover, using the new culture conditions we demonstrate that alternative promoter choice regulating the expression of the master transcription factor Blimp-1/Prdm1 can be observed; when the canonical B cell promoter for *Prdm1* is deleted, differentiating B cells exhibit flexibility in the choice of promoter, dictated by the initiating stimulus, with preferential maintenance of expression following exposure to TLR ligation. Thus our system provides a readily tractable model for furthering our understanding of plasma cell biology. ***The Journal of Immunology*****, 2022, 208: 514–525.**

Following antigenic encounter, B cells alter their physiological state and initiate a differentiation process that ultimately produces Ab-secreting cells (ASCs). The activation of B cells can be separated into two pathways based on the type of Ag and whether it requires the presence of T cells to elicit an immune response. T cell–independent Ags such as bacterial LPS and polymeric proteins stimulate B lymphocytes through TLR activation or BCR crosslinking. In contrast, a T cell–dependent response arises from B cells binding to a protein Ag, followed by cognate interaction with follicular helper T cells. Initially, an extrafollicular pathway produces short-lived Ab-secreting plasmablasts with moderate affinity. Secondary signals such as CD40 engagement are vital to the formation of germinal centers where somatic hypermutation leads to higher affinity Abs (1–3). Consequently, thousands of memory B cells and plasma cells emerge, providing a range of Ag-specific effector cell types (4, 5).

ASC is a broad term that encompasses both short-lived cycling plasmablasts and long-lived quiescent plasma cells that reside in specialized niches, primarily within the bone marrow (6). During recent years, optimization of human B cell differentiation conditions has resulted in the in vitro generation of long-lived plasma cells, capable of surviving in culture for extended periods of time (7–10). This has resulted in the ability to sequentially explore and manipulate each stage of differentiation.

To the best of our knowledge, a murine counterpart system does not exist. There are many variations of murine in vitro ASC generation (11), but the most commonly described technique uses the TLR4 agonist, bacterial LPS. To enhance B cell activation, T cell help can be included in the form of costimulatory proteins (CD40L) and cytokines (IL-4 and IL-5) (12). These approaches are effective for modeling partially differentiated, short-lived plasmablasts, but fail to generate terminally differentiated plasma cells that can be sustained as a quiescent population in vitro. In support of this, work by Shi and colleagues demonstrated that the gene expression profile of in vitro–derived ASCs stimulated using CD40L, IL-4, and IL-5 for 5 d was as different from fully mature plasma cells as it was from activated B cells (13). The inability to generate long-lived plasma cells means that studies of normal murine plasma cell biology are limited in an in vitro setting. An example of this is the ability to track the relationships between signaling pathways and transcriptional control in a continuously differentiating population. A gene for which this may be particularly relevant is *Prdm1*. The expression of *Prdm1* encoding the transcription factor Blimp-1 is essential for the changes in gene expression that accompany the generation of ASCs (14). Previous work has suggested that transcription of *Prdm1* in ASCs is strictly governed by a promoter initiating in exon 1A (15), which is maintained in a primed accessible state in naive B cells (16).

*Division of Haematology and Immunology, Leeds Institute of Medical Research, University of Leeds, United Kingdom; and †Haematological Malignancy Diagnostic Service, St James's Institute of Oncology, Leeds, United Kingdom

ORCIDs: 0000-0001-6584-5889 (M.A.C.); 0000-0002-6694-2979 (K.W.); 0000-0003-2915-7119 (R.M.T.); 0000-0003-0665-6759 (G.M.D.).

Received for publication January 7, 2021. Accepted for publication October 29, 2021.

This work was supported by Cancer Research UK program grants C7845/A17723 and C7845/A29212.

E.R. designed and performed experiments, analyzed data, and wrote the paper; M.A.C. performed bioinformatic analysis; K.W. performed experiments and analyzed data; M.C. assisted with experiments and data analysis; R.M.T. contributed to experimental design, data analysis, and writing the paper; G.M.D. designed experiments, analyzed data, wrote the paper, and oversaw the project. All authors participated in editing the paper.

The sequences presented in this article have been submitted to National Center for Biotechnology Information Gene Expression Omnibus (https://www.ncbi.nlm.nih.gov/geo/query/acc.cgi) under accession number GSE160823.

Address correspondence and reprint requests to Dr. Gina M. Doody, University of Leeds, Leeds Institute of Medical Research, St. James's University Hospital, Leeds, West Yorkshire LS9 7TF, U.K. E-mail address: g.m.doody@leeds.ac.uk

The online version of this article contains supplemental material.

Abbreviations used in this article: ASC, Ab-secreting cell; EdU, 5-ethynyl-2′-deoxyuridine; MDS, multidimensional scaling; PGCNA, parsimonious gene correlation network analysis; RNA-seq, RNA-sequencing; VST, variance stabilizing transformation; WT, wild-type.

www.jimmunol.org/cgi/doi/10.4049/jimmunol.2100004

To address this issue, we have adapted two model systems used for human (9) and murine (17) B cell differentiation. Following additional optimization, two methods of plasma cell generation using LPS-induced TLR signaling or Ab-induced BCR signaling in conjunction with CD40L and cytokines were achieved. The plasma cells generated in each condition were validated to ensure characteristics such as quiescence and phenotypic markers along with gene expression profile were consistent with in vivo murine plasma cells. Using our newly developed models, we demonstrate that *Prdm1* can be generated in the absence of exon 1A, giving rise to plasma cells in culture, despite a reduction in the levels of this key transcript and an altered gene expression profile in exon 1A–deleted cells.

Materials and Methods

B cell isolation

Spleen tissue was harvested from sex- and age-matched C57BL/6, Blimp-1–Venus (18) or *Prdm1*$^{\Delta ex1A}$ mice (15) (kindly provided by E. Bikoff and E. Robertson, University of Oxford) between 6–12 wk old that had been maintained in specific pathogen–free conditions. All procedures were performed under the approved U.K. Home Office project license in line with the Animal (Scientific Procedures) Act 1986 and in accordance with the U.K. National Cancer Research Institute Guidelines for the welfare of animals. Single-cell suspensions were obtained after density centrifugation using lympholyte-M (Cedarlane). The EasySep Mouse B Cell Isolation Kit (STEMCELL Technologies) containing anti-CD43 was used to isolate B2 cells. Following isolation, B cells were phenotyped to ensure >95% purity before culture.

Optimized culture conditions

Day 0. For BCR signaling, isolated B cells were seeded in 24-well plates at 2.5×10^5 cells per milliliter (0.5 mL per well; 1.25×10^5 cells per well) with irradiated CD40L-expressing murine L cells (0.5 milliliter per well; 6.25×10^4 cells per well), 12 μg/ml F(ab′)$_2$ anti-IgM/IgG (Jackson Immuno Research Labs), 50 ng/ml IL-4, and 50 ng/ml IL-5 (Miltenyi Biotech) in IMDM media containing 10% FCS and 50 μM β-mercaptoethanol for 2 d.

For TLR signaling, B cells were seeded at the same density as above with CD40L-expressing murine L cells, 5 μg/ml LPS (0111:B4; Sigma-Aldrich), IL-4, and IL-5.

For LPS-alone stimulations, 5 μg/ml LPS was used without cytokines or CD40L.

Day 2. On subsequent days, both mechanisms followed the same steps. At day 2, cells were removed from the CD40L cells and transferred across to new 24-well plates.

Day 4. On day 4, plasmablasts were reseeded in 10 ng/ml IL-6 (Miltenyi Biotech), 100 ng/ml APRIL (Caltag), MEM amino acids and Lipid Mixture 1 (Sigma-Aldrich) at 5×10^5 cells per milliliter in 96-well plates (0.2 milliliter per well; 1×10^5 cells per well). Cells were fed with fresh media every 3–4 d containing APRIL, IL-6, amino acids, and lipids. Feeding was carried out until elective termination.

Flow cytometric evaluation. Cells were incubated with Fc block (BD Biosciences) prior to staining with Abs to B220 (PE-conjugated clone RA3-6B2; Miltenyi Biotech) and CD138 (allophycocyanin-conjugated clone REA104; Miltenyi Biotech). 7-AAD was added immediately before samples were analyzed using a CytoFLEX S (Beckman Coulter). Absolute cell counts were performed with CountBright beads (Invitrogen). Blimp-1 expression was monitored throughout the differentiation using a 525/40 bandpass filter. Cell division was assessed using 5-ethynyl-2′-deoxyuridine (EdU; Invitrogen) or Ab to Ki67 (Clone B56 [RUO] Alexa Fluor 488 Mouse Anti–Ki-67 FITC; BD Biosciences). Cells were incubated with either 1.5 μM EdU for 24 h or 10 μM EdU for 2 h prior to processing with the Click-iT EdU Kit (Alexa Fluor 647; Thermo Fisher Scientific) following the manufacturer's protocol on the day of staining. Alternatively, cells were fixed, permeabilized and stained with anti-Ki67. Cells were stained with a live/dead dye prior to fixation (Zombie Ultraviolet Fixable Viability Kit; BioLegend). All data were analyzed using FlowJo software (v. 10; BD Biosciences).

Ig quantification. ELISAs were performed according to the manufacturer's instructions for the Mouse IgM Quantification Set (E90-101; Bethyl Laboratories) or Mouse IgG Quantification Set (E90-131; Bethyl Laboratories). The concentrations were measured using a plate reader (Cytation 5; BioTek Instrument) and standard curve analysis software (ELISAkit).

Gene expression. RNA was obtained using TRIzol (Invitrogen) and sequencing libraries generated with a TruSeq Stranded Total RNA Human/Mouse/Rat Kit (Illumina). Libraries were sequenced on a NextSeq500 platform (Illumina), using 76-bp single-end sequencing. The fastq files were assessed for initial quality using FastQC v. 0.11.8 (https://www.bioinformatics.babraham.ac.uk/projects/fastqc/), trimmed for adapter sequences using TrimGalore v. 0.6.0 (https://www.bioinformatics.babraham.ac.uk/projects/trim_galore/) and aligned to GRCm38.p6/mm10 (Gencode release M20) using STAR aligner (v. 2.6.0c) using twopassMode (19–22). Transcript abundance was estimated using RNA-*Seq* by Expectation-Maximization v. 1.3.0 and imported into R v. 3.5.1 using txImport v. 1.10.1 and then processed using DESeq2 v. 1.22.2 (20–22). Using DESeq2 variance stabilizing transformation (VST) transformed data, exploratory analysis was carried out using multidimensional scaling (MDS) (all genes). Differential gene expression was determined using DESeq2, quality visualized using MA plots and shrinkage of log fold estimated using the apeglm method (23). VST transformed data were exported for downstream visualizations using the GENE-E package (v. 3.0.21; https://software.broadinstitute.org/GENE-E/).

The data from Shi et al. (13) (GEO GSE60927) were downloaded from the Sequence Read Archive and processed with the same RNA-sequencing (RNA-seq) pipeline, merged with the in vitro generated time course data and any batch effects removed using ComBat (R SVA package) (24) before visualization with MDS and GENE-E.

Details of parsimonious gene correlation network analysis (PGCNA) network analysis have been described elsewhere (25). Briefly, Spearman rank correlations were calculated for all gene pairs and correlation matrices clustered using the fast unfolding of communities in large networks algorithm (version 0.3). The overlap of the modules of correlated genes between the networks at the gene and signature level was assessed using a hypergeometric test and visualized as heatmap using the Broad GENE-E package (https://software.broadinstitute.org/GENE-E/). Data were hierarchically clustered (Pearson correlations and average linkage) and signature enrichments were filtered to false discovery rate <0.1 and ≥ 5 and ≤ 1500 genes for the signature sets, selecting the top 30 most significant signatures per module.

The D0-D10 TLR/BCR and D0-D7 LPS/TLR/BCR (wild-type [WT]/Δ*ex1A*) samples were used to generate two input data sets for PGCNA analysis by selecting genes differentially expressed (false discovery rate < 0.05) either temporally or between conditions. This resulted in TLR/BCR and LPS/TLR/BCR data sets of 15,245 and 15,887 genes respectively which were analyzed with pgcna2 [settings -n 1000, -f 1, -b 100] (https://github.com/medmaca/PGCNA/tree/master/PGCNA2) (25).

Statistical analysis of differential exon usage of *Prdm1* transcripts was performed using the DEXSeq integrative R package (v. 1.30) (26), visualizing relative exon usage (splicing = TRUE; i.e., remove overall expression changes).

Results

Production of phenotypically mature murine plasma cells in vitro

ASCs generated in culture typically express the differentiation-associated marker CD138 and maintain the B cell marker B220 (27), however fail to terminally differentiate into plasma cells characterized by loss of the B220 marker (Fig. 1A) and exit from cell cycle. Although the introduction of additional ligands such as APRIL, demonstrably enhance the production of ASCs (17), such protocols limit the exposure of B cells to a single round of stimuli. To encourage differentiation past the plasmablast stage, alternative combinations of cytokines were tested in a multistep culture based on a model of human plasma cell differentiation shown to promote the long-term maintenance of plasma cells (9). This culture consists of three stages: 1) commitment to differentiation through initial stimulation in the presence of CD40L, 2) removal of CD40L to enable expansion of activated B cells, and 3) maturation of plasma cells using niche-like factors such as IL-6 and APRIL. We systematically tested the effect of different combinations at each stage to determine suitability for murine B cells assessing phenotypic profiles and cells numbers throughout the culture period. Cells were initially cultured with CD40L, F(ab′)$_2$ anti-IgM/IgG or LPS and combinations of IL-21, IL-2, IL-4, and IL-5. Cells were then removed from CD40L-expressing fibroblasts at day 2 and kept in the original cytokines. At day 4, cells were resuspended in IL-6 and APRIL and refed every 3 d (Fig. 1B).

Once TLR (LPS/CD40L/IL-4/IL-5)- and BCR (anti-Ig/CD40L/IL-4/IL-5)-stimulating conditions had been optimized, a direct comparison of the two systems was performed. On day 4, populations appeared

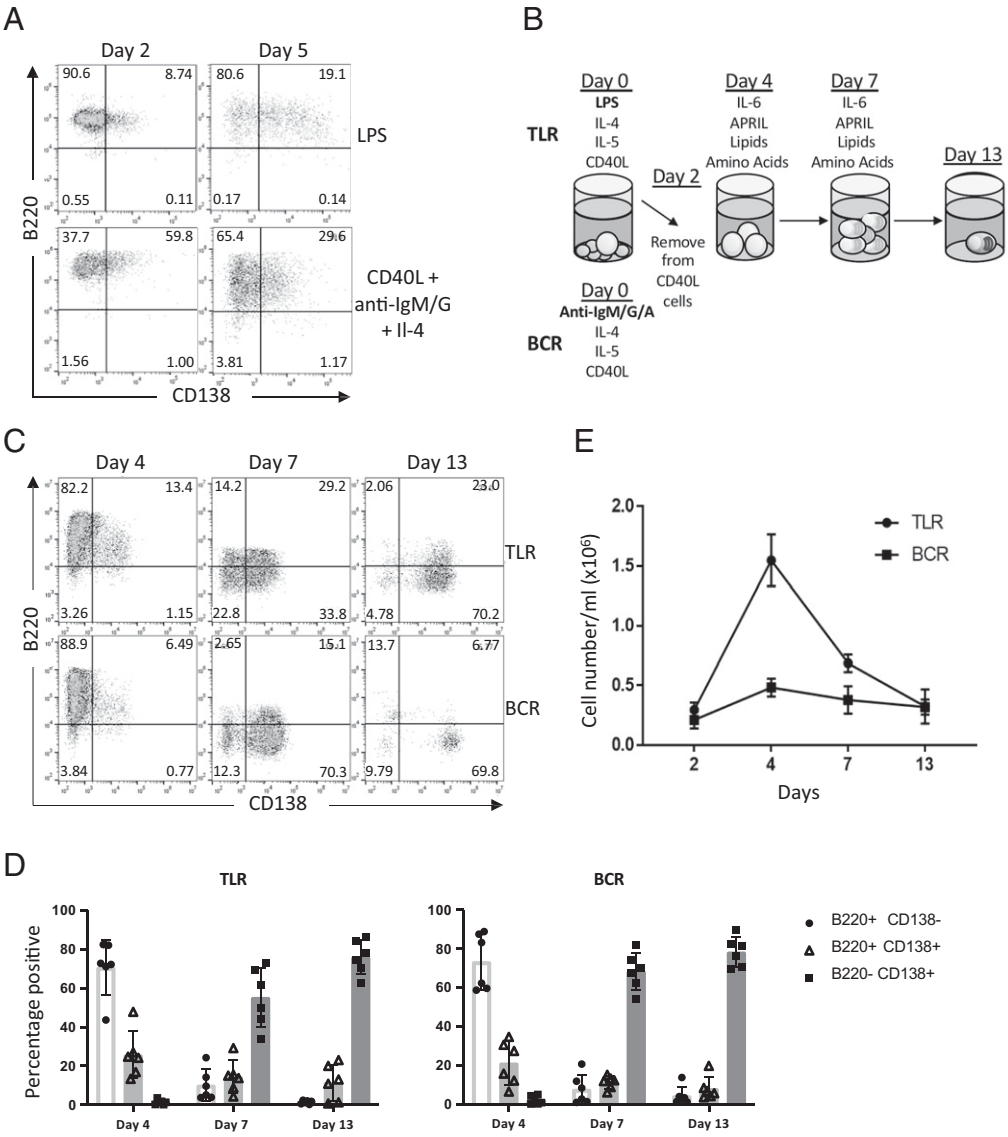

FIGURE 1. Generation of phenotypically mature plasma cells using TLR and BCR stimulation conditions. (**A**) Purified splenic B cells were resuspended in conditions including LPS or CD40L + $F(ab')_2$ anti-IgM/IgG + IL-4 for 5 d. On days 2 and 5, cells were phenotyped using Abs to B220 and CD138. (**B**) Schematic of in vitro differentiation conditions using either TLR- or BCR-initial stimuli. (**C**) B cells were resuspended in CD40L, LPS, IL-4, and IL-5 (TLR) or CD40L, $F(ab')_2$ anti-IgM/IgG, IL-4, and IL-5 (BCR). On day 2, cells were removed from CD40L and transferred to a fresh plate. On day 4, cells were reseeded in IL-6 and APRIL. Cells were phenotyped on the indicated days using Abs to B220 and CD138. Representative flow plots are shown. (**D**) Percentage of B cells ($B220^+CD138^-$), plasmablasts ($B220^+CD138^+$) and plasma cells ($B220^-CD138^+$) from six independent differentiations. Averages ± SD are shown on the plots. (**E**) Cell number was recorded throughout the differentiation. Results are displayed as the mean ± SD for three individual mice and are representative of at least three independent experiments.

similar to one another although there was a decreased percentage of cells expressing $B220^+CD138^+$ following BCR stimulation (Fig. 1C, 1D). On day 7, overall populations were still comparable; however, cells stimulated with BCR conditions appeared as a more discrete population with slightly higher CD138 expression. By day 13, cells generated using TLR stimuli were more discrete but still demonstrated much lower CD138 expression than BCR-stimulated cells. Cell counts revealed that a high degree of proliferation occurred between day 2 and 4 using TLR stimuli, which was reduced in cells generated using BCR conditions (Fig. 1E). Following the proliferative phase, cell number decreased. By day 13, cell number was comparable in both conditions.

Tracking indicative features of mature plasma cells

Blimp-1 is a transcriptional repressor able to drive the terminal differentiation of B cells into Ig-secreting plasma cells (28). To confirm Blimp-1 upregulation during culture, *Blimp-1* Venus reporter mice were used (18). Isolated B cells were cultured in both TLR and BCR conditions and Blimp-1 expression was tracked over the course of 13 d using flow cytometry (Fig. 2A). Blimp-1 expression increased significantly between day 4 and day 7/day 9, consistent with the generation of a $B220^-CD138^+$ plasma cell population.

The key difference between a plasmablast and plasma cell is the cessation of cell cycle (29). With this in mind, it was important to assess proliferative capacity during both models of in vitro differentiation. Cells were loaded with EdU (5-ethynyl-2′-deoxyuridine) at different time points and the degree of incorporation assessed (Fig. 2B). At day 4, when peak cell numbers were obtained, a 2-h pulse of EdU in the culture labeled ∼30% of the cells in either condition. Prolonged exposure to EdU (24 h) before sampling demonstrated that around 80% of the cells had proliferated between day 3 and day 4. Following incubation of day 7 cells with EdU, less than 1% incorporation was observed at day 8 and this was recapitulated by the 2-h pulse label, suggesting that cells lose proliferative capacity from that point. As additional evidence to support cessation of cycling, cells were also stained with anti-Ki67, which showed similar profiles to the EdU incorporation (Fig. 2B) To relate the decline in proliferative capacity to the acquisition of the plasma cell state, phenotypic profiles were analyzed over a 4-d time course. Between days 7 and 8, there was a change in CD138 distribution to form a discrete plasma cell population (Fig. 2C). After this, the phenotype remained stable suggesting that establishment of the plasma cell population and cell cycle exit occur concurrently.

As plasma cells have the functional ability to secrete Ig, it was also important to determine whether phenotypically maturing cells could both secrete and class switch. Supernatants were collected at days 4, 7, and 10 and analyzed using an ELISA (Fig. 2D). At day

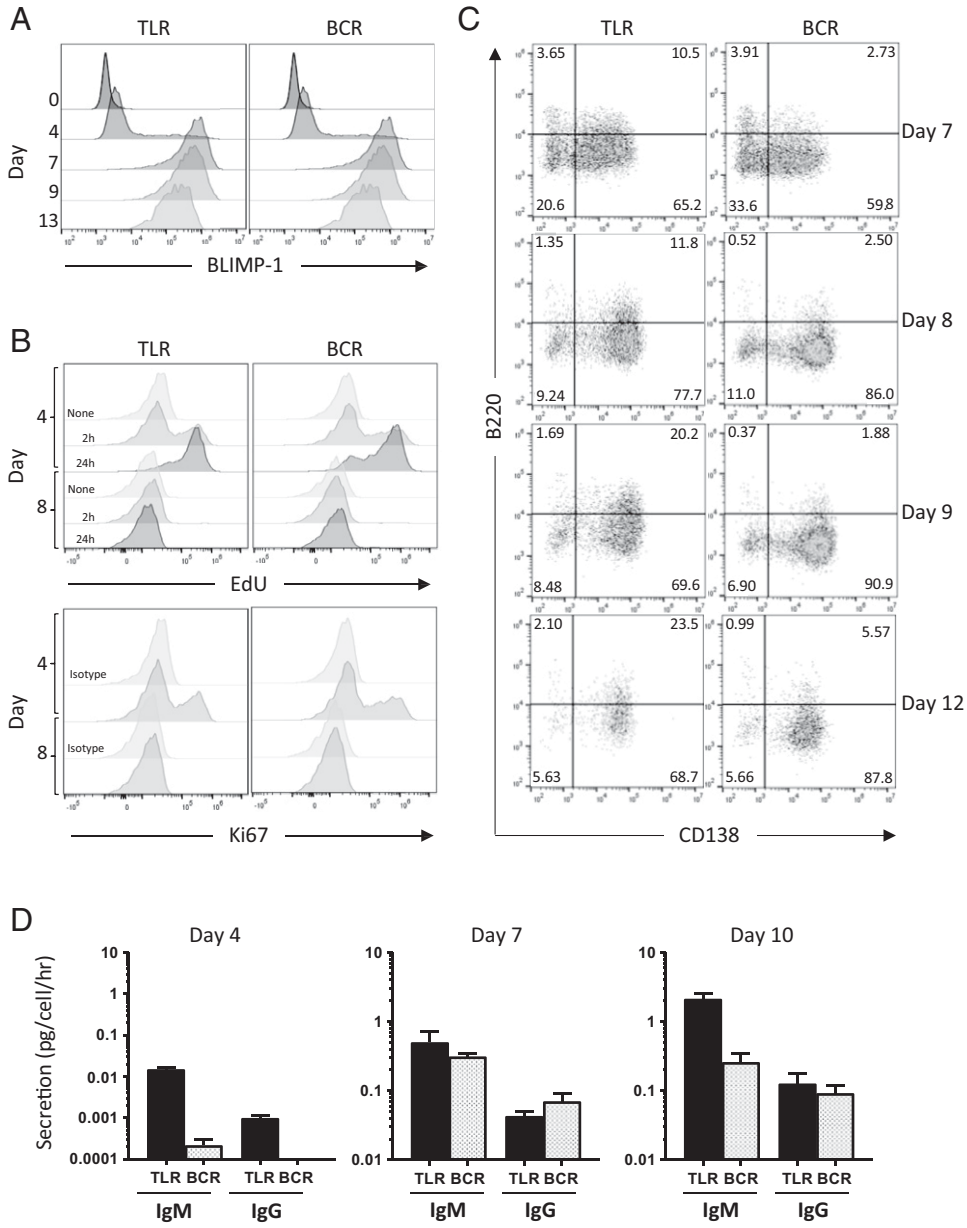

FIGURE 2. In vitro generated plasma cells display characteristic features of maturation. (**A**) Purified splenic B cells from *Blimp1-Venus* reporter mice cultured in either TLR and BCR conditions were analyzed using flow cytometry on day 0, 4, 7, 9, and 13 for Blimp-1 expression. Plots are representative of two independent experiments each performed with three mice. (**B**) Cells derived from WT mice were incubated with EdU for either 24 or 2 h and assessed on day 4 or 8 using flow cytometry. Cells from the same cultures were also stained with anti-Ki67. Plots are representative of two independent experiments. (**C**) Phenotypic evaluation of differentiating cells at the transition to cell cycle exit. (**D**) Supernatant was collected at day 4, 7, and 10 from in vitro cultures. IgM and IgG concentrations were quantified using an ELISA and normalized using cell counts and the amount of time in culture. Results are displayed as the mean ± SD for three individual mice.

4, levels of Ig secretion were low as would be expected. TLR conditions promoted a small degree of IgM secretion and even less IgG, whereas BCR conditions resulted in barely detectable levels of both IgM and IgG. At day 7, both TLR and BCR conditions promoted high levels of IgM and lower levels of IgG. At day 10, TLR conditions promoted even higher levels of IgM whereas BCR conditions produced similar amounts to day 7. IgG increased in both conditions between days 7 and 10 but still remained comparatively lower.

Transcriptional profiling of in vitro–generated plasma cells

The differentiation of activated B cells into ASCs requires coordinated changes in the expression of many hundreds of genes and the data from Shi et al. (13) convincingly demonstrates that current in vitro protocols fail to generate cells that match bone marrow–derived long-lived plasma cells. To provide evidence that the transcriptome of ASCs generated using the TLR and BCR conditions exhibited progressive plasma cell characteristics, gene expression profiling was performed at multiple time points across the system (days 0, 4, 7, and 10).

Gene expression profiling of individual loci appeared to suggest that late time points are indeed plasma cell–like in both BCR and TLR conditions, with high expression of genes such as *Irf4, Prdm1*, and *Xbp1* and the reciprocal loss of *Irf8*, *Bach2*, and *Pax5* (Fig. 3A). Furthermore, plasma cells appeared distinct from the in vitro versions demonstrated by Shi and colleagues and instead displayed a common gene program consistent with bone marrow plasma cells (13). Notably, this includes the extinction of genes associated with proliferation such as *Foxm1* and *Mki67*. MDS evaluation of similarity confirmed that the TLR and BCR generated plasma cells have a gene expression profile in keeping with full differentiation, surpassing the other in vitro conditions in resembling bone fide, long-lived plasma cells (Fig. 3B).

Although both conditions led to the production of mature plasma cells, the different types of input signals are likely to generate nuanced versions of the core plasma cell gene expression program. To determine the effect of TLR versus BCR, PGCNA (25) was performed on the differentially expressed genes over time (Fig. 4A). In total, 24 modules of coexpressed genes were identified that could be linked to gene signature and ontology term enrichments. As anticipated, freshly isolated day 0 cells exhibited a gene expression profile

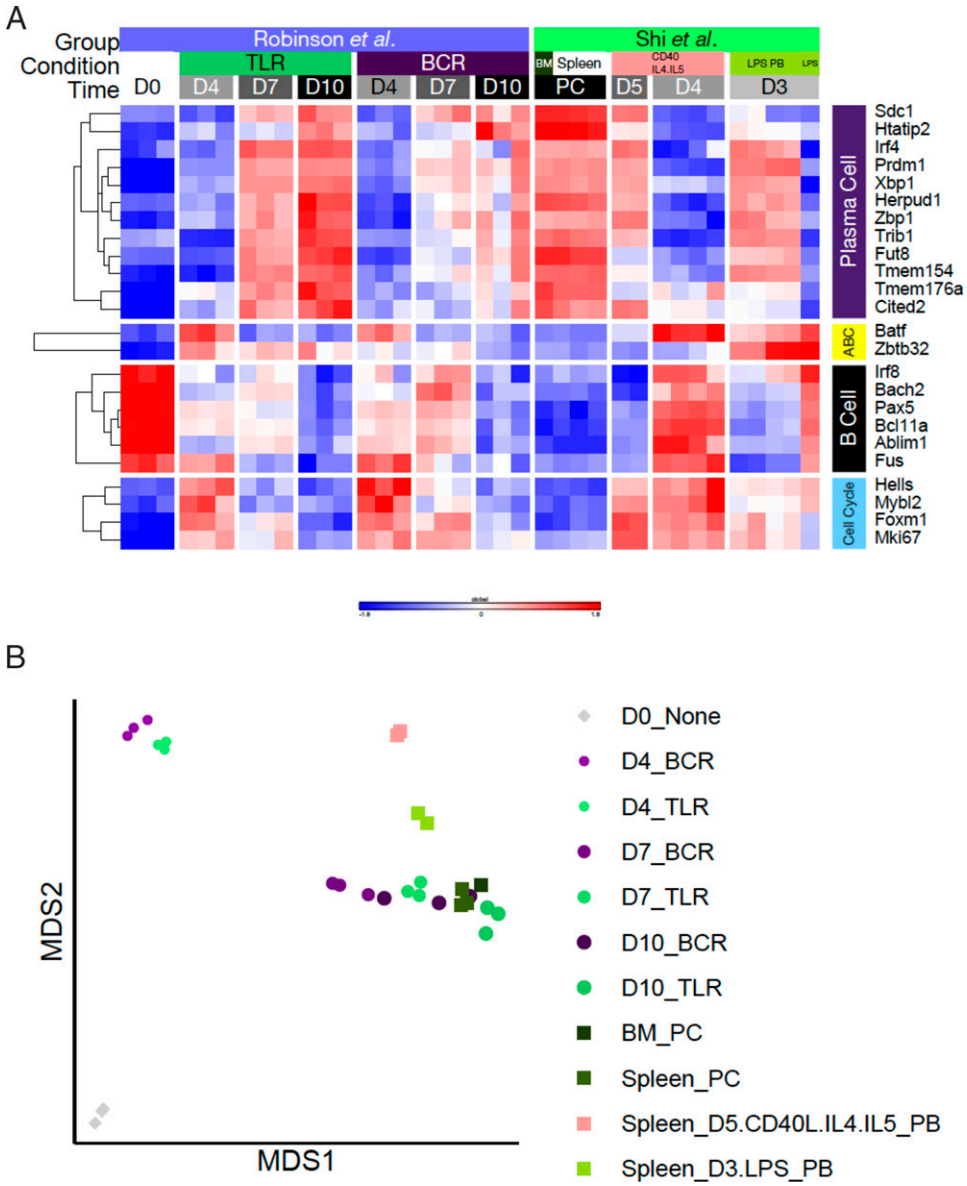

FIGURE 3. Transcriptomic profiling of in vitro generated plasma cells. (**A**) Purified splenic B cells were stimulated with BCR or TLR conditions. On day 0, 4, and 7 and 10, RNA was isolated from three samples for each condition and sequenced. These data were merged with that from Shi et al. (15) (GSE60927) and ComBat normalized to remove batch effects. VST-normalized expression values of genes are displayed as a heatmap on a *z*-score scale. (**B**) MDS analysis of samples in (A).

typical of a naive B cell population that dramatically shifted after exposure to either condition (Fig. 4B, 4C). By day 4 both types of stimulation resulted in the loss of M13: NaiveBcell and gain of modules related to translational processes (M8: Ribosome, M3:RNA_ProcessingRibosome_biogenesis), cell cycle (M10: CellCycle), and metabolic reprogramming (M11: MitochondriaOxPhos, M16: MitochondriaOxPhos_2), consistent with the requirements for increased growth. By day 4, diverging gene expression patterns also began to emerge: BCR elicited a more pronounced increase in M2: EMT_Matrisome_StemLike and marked extinction of M22: IFN, whereas TLR enhanced the expression of genes associated with M19: ATF4. At day 7 as the cells are transiting through the plasmablast stage, those exposed to BCR conditions continue to maintain higher levels of M2: EMT_Matrisome_StemLike, whereas TLR conditions promote the acquisition of modules most directly associated with the ASC phenotype (M21: Ig, M18: XBP1_UPR Golgi_PlasmaCell, M1: Golgi_Lysosome, M20: Golgi_XBP1). A distinct feature of the cells obtained at day 10 was the augmented expression of M2: EMT_Matrisome_StemLike and M5: Lymphnode_Matrisome following culture with agonists of the BCR. Among the genes that feature in these modules include extracellular matrix components such as the secreted glycoprotein *Fbln2*, the matricellular collagen-binding protein *Sparc* and multiple collagen family members (Fig. 4D). Overall, ASCs generated using TLR or BCR conditions progressively acquire a mature plasma cell transcriptome, but display unique signatures at the later time points intimating that the initial signals generate nonequivalent plasma cell populations.

Prdm1 *transcript initiation is coupled to the nature of differentiation stimulus*

A specific reason for developing this model system was the potential application to interrogate detailed features of plasma cell differentiation in genetic models. With a validated model of murine plasma cell differentiation in place, the next step was therefore to test the hypothesis that the system could provide novel insight into plasma cell biology using genetic models. Previous work by Morgan et al. (15) has shown that the mouse *Prdm1* gene has three alternative promoter regions (1A, 1B, and 1C), which could play important roles in generating regulatory diversity (Fig. 5A).

Deletion of exon 1A (Δ*ex1A*) leads to the loss of Blimp-1 expression in LPS-treated splenocytes and defective IgM secretion (15), supporting the conclusion that exon 1A is essential for Blimp-1

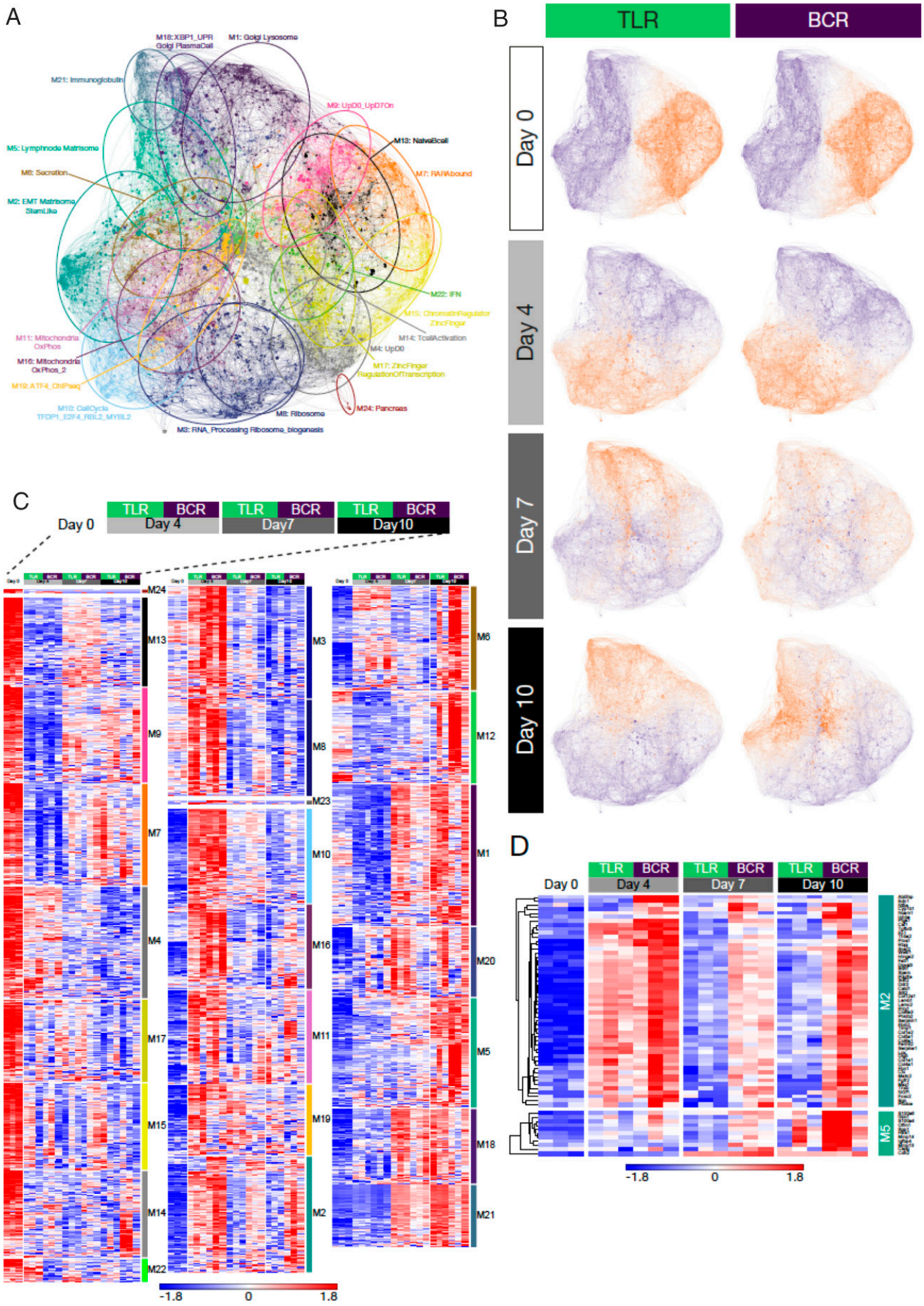

FIGURE 4. Network analysis of gene expression programs during in vitro plasma cell differentiation. (**A**) PGCNA of gene expression derived from murine splenic B cells cultured in TLR or BCR conditions. Network comprises 24 modules; signature enrichment analysis was used to determine biological features of individual modules and derive representative summary terms. (**B**) Overlay of gene expression *z*-scores for genes in the network *(Figure legend continues)*

expression in the B cell lineage. However, in the absence of exon 1A other cell lineages can still generate moderate to normal levels of Blimp-1, raising the possibility that *Prdm1* may be differentially transcribed dependent upon signaling cues or cellular context. To investigate this further, the effect of exon 1A deletion on both TLR and BCR generated plasma cells was assessed. B2-B cells were isolated from WT and Δ*ex1A* mice and cultured in LPS alone, TLR, or BCR conditions.

Upon stimulation with LPS alone, day 4 results supported the observation of Morgan and colleagues after a 3-d culture, with more of the WT cells displaying a phenotype consistent with differentiation than the Δ*ex1A* cells (Fig. 5B). However, extending the duration of culture provided a different perspective and by day 7, a proportion of the Δ*ex1A* derived cells were phenotypically more plasma cell-like than the WT counterparts. Cell number was also higher in the Δ*ex1A* cells throughout the differentiation (Fig. 5C).

Differentiation was further assessed using the enhanced culture system comparing culture in TLR or BCR conditions to establish whether differentiation conditions impacted on plasma cell generation in the presence or absence of exon 1A. Under TLR conditions, Δ*ex1A* cells were able to generate plasma cells similar to WT, although there was a decrease in cell number by day 7 (Fig. 5B, 5C). In contrast, under BCR conditions, Δ*ex1A* cells failed to generate a substantial plasma cell population by day 7, with the majority of the population negative for both B220 and CD138, accompanied by a reduction in cell number. Assessment of Ig production confirmed that Δ*ex1A* cells increased secretion over time and that when cell number was considered, cells that survived under BCR conditions were still capable of Ab production (Fig. 5D).

As cells were able to differentiate under TLR conditions, it seemed plausible that Δ*ex1A* cells could potentially use an alternative *Prdm1* promoter to initiate transcription. This was addressed using RNA-sequencing and analysis using DEXSeq (26) to compare the composition of transcripts between WT and Δ*ex1A* cells. First, regardless of stimulating condition, there were transcripts that originate from exon 1A in WT mice, which were absent in Δ*ex1A* mice (Fig. 6A, Supplemental Fig. 1) confirming the efficacy of the deletion on transcripts initiating from this promoter and exon. In all samples there were also transcripts whose origin was mapped to exon 2, which would be consistent with regulation by the exon 1C promoter. Δ*ex1A* mice showed additional transcript variants originating upstream of exon 1A consistent with regulation by the exon 1B promoter, most prominently in the TLR conditions at day 7, which were not present in WT samples (Supplemental Fig. 1). Furthermore, there was evidence of the previously described splice variant Δexon 6 (previously referred to as exon 7 in published literature) (30–32).

Deletion of exon 1A also affected overall expression of *Prdm1*. Δ*ex1A* cells cultured in LPS or BCR conditions demonstrated lower expression of *Prdm1* at day 4 in comparison with WT cells, whereas Δ*ex1A* cells cultured in TLR conditions expressed levels equivalent to the WT (Fig. 6B). However, at the day 7 time point even the Δ*ex1A* cells in TLR conditions expressed significantly lower levels of *Prdm1*. These data confirm that exon 1A is important for optimal expression of *Prdm1* in the B cell lineage, but additionally demonstrate that dependence on this particular promoter and initiating exon is linked to the nature of the extracellular cue initiating differentiation.

Prdm1 *transcript/stimulus coupling is functionally linked to differentiation*

To ascertain how the coupling between differentiation stimulus and Δ*ex1A* dependence impacted on the execution of the plasma cell program, gene expression was evaluated on days 4 and 7 of culture. As suggested by the phenotypic analysis, Δ*ex1A* cells stimulated with LPS lagged behind the WT cells at day 4, but were similar in the overall gene expression by day 7 (Fig. 7A). Δ*ex1A* cells obtained in either TLR or BCR conditions at day 4 were comparable to WT cells. By day 7 Δ*ex1A* cells grown in TLR conditions had moved considerably closer to the expected plasmablast/plasma cell gene expression profile, but BCR stimulated Δ*ex1A* cells failed to mature beyond an activated B cell state. Overall, these data are consistent with models that demonstrate an absolute requirement for Blimp-1 expression for differentiation after the activated B cell state. Under BCR stimulated conditions this transition requires an intact exon 1A promoter, by contrast LPS can drive compensatory expression of *Prdm1* from alternative promoters thus allowing differentiation to proceed.

To explore the gene expression profile of the Δ*ex1A* cells in more detail, PGCNA was applied. The network generated using LPS-, TLR-, or BCR-stimulated WT and Δ*ex1A* cells yielded 16 modules of coexpressed genes linked to gene signature and ontology term enrichments (Supplemental Fig. 2). Despite phenotypic maturation and overall apparent similarity of Δ*ex1A* cells to WT in cells exposed to a TLR agonist, there were notable differences in several of the modules (Fig. 7B, Supplemental Fig. 3). For example, in terms of modules that are initially expressed in B cells, the two related modules M1: SMARCA2_UP UV_RESPONSE_DN Zinc-Finger Ubl_ConjugationPathway and M2: HAPTOTAXIS SMARCA2_UP UV_RESPONSE_DN EZH2_TARGETS_DN feature genes that are rapidly repressed after LPS stimulation and repressed by either TLR or BCR stimulation in Δ*ex1A* cells at day 7 but maintained in WT. Additionally, the module M5: MemoryBcell BoundByFOXP3 was repressed in all cell types at day 4. This repression was retained in LPS-stimulated as well as TLR- or BCR-triggered Δ*ex1A* cells at day 7, whereas module genes came back on at day 7 in response to TLR or BCR conditions in WT.

There were equally apparent differences for modules acquired as the Δ*ex1A* cells became more plasma cell like following differentiation with LPS alone. In particular there were marked deficiencies in the ability of Δ*ex1A* cells to regulate genes belonging to modules M3:Ribosome RibosomeBiogenesis Mitochondria CellCycle OxPhos EZH2_TARGETS_UP, M7: Chr19p13q13 EZH2_TARGETS_UP, and M13: Matrisome LymphNode StemLike. For example, dysregulation of *Phgdh*, *Eno1*, and *Gapdh*, three functionally linked glycolytic enzymes in module M3 suggests that lower levels of Blimp-1 are impacting on metabolic fitness and the acquisition of Ig-CAM adhesion molecules in M13 such as *Icam1*, *Bcam*, and *Epcam* argues for altered adhesive properties.

In keeping with the failure of Δ*ex1A* cells stimulated with BCR conditions to upregulate *Prdm1* and achieve phenotypic maturation, several modules showed defects for these samples. Among these include modules associated with increased Ig production such as M10:PC Golgi XBP1bound ER_UPR ProteinSecretion and M6: PC IRF4_Induced XBP1bound ER_UPR Ig, consistent with the described role for Blimp-1 in murine plasma cells (14).

shown in blue (low) to red (high) *z*-score color scale. Conditions are indicated above the network images with time point of sampling to the side. (**C**) Module expression values illustrated as heatmap showing the expression across three independent differentiations per time point. At each time point, samples are grouped according to stimulation with TLR (left) or BCR (right). (**D**) Selected gene expression from modules M2 and M5.

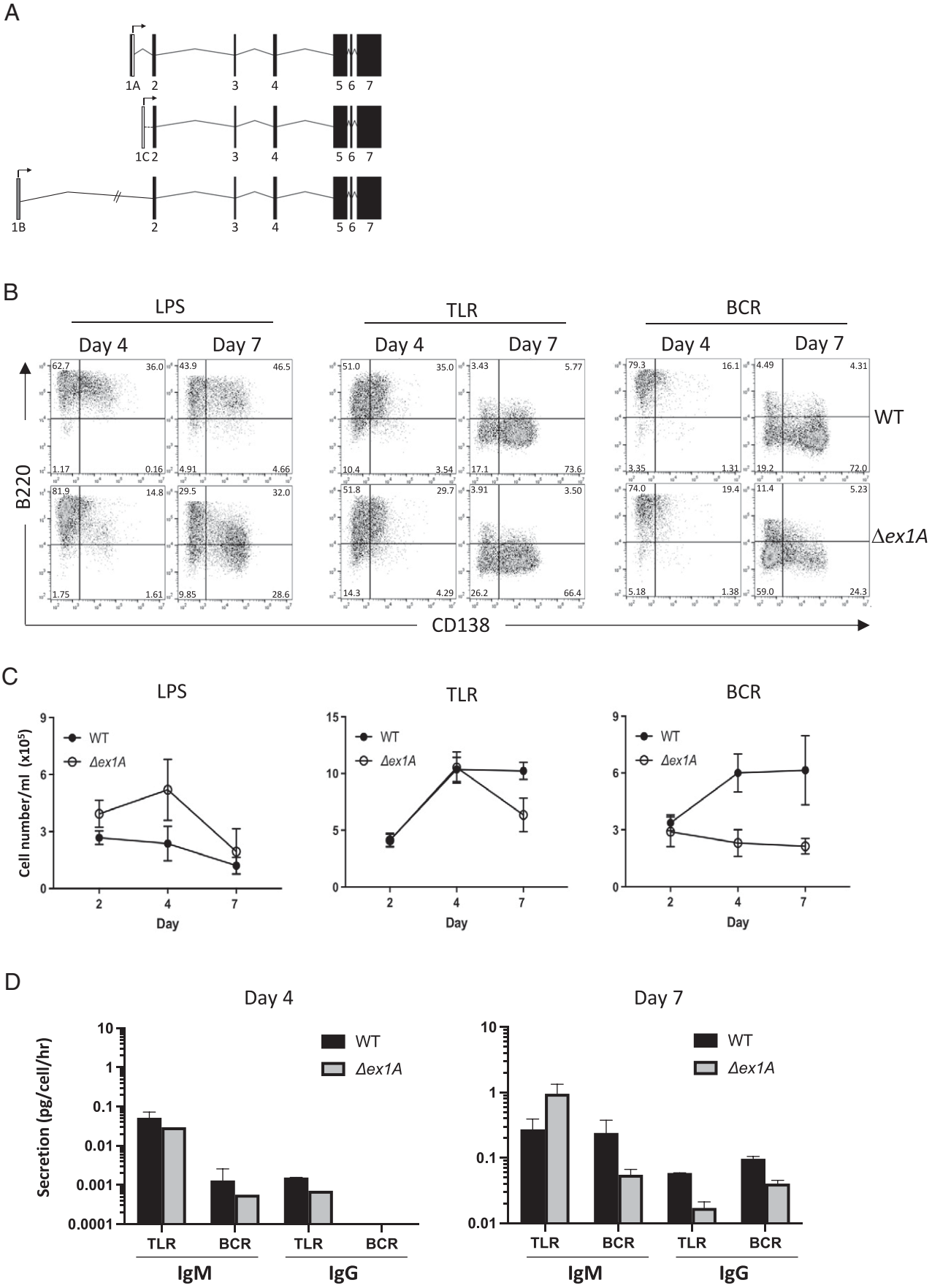

FIGURE 5. TLR and BCR stimulation conditions generate phenotypic ASCs from mice lacking the *Prdm1* exon 1A regulatory region. (**A**) Schematic of *Prdm1* alternative promoters 1A, 1B, and 1C based on Morgan et al. (15) with exon numbered according to RefSeq annotation. Black arrows indicate transcription start sites. The alternative first exon, exon 1B, and the previously characterized exon 1A both splice directly to exon 2. *(Figure legend continues)*

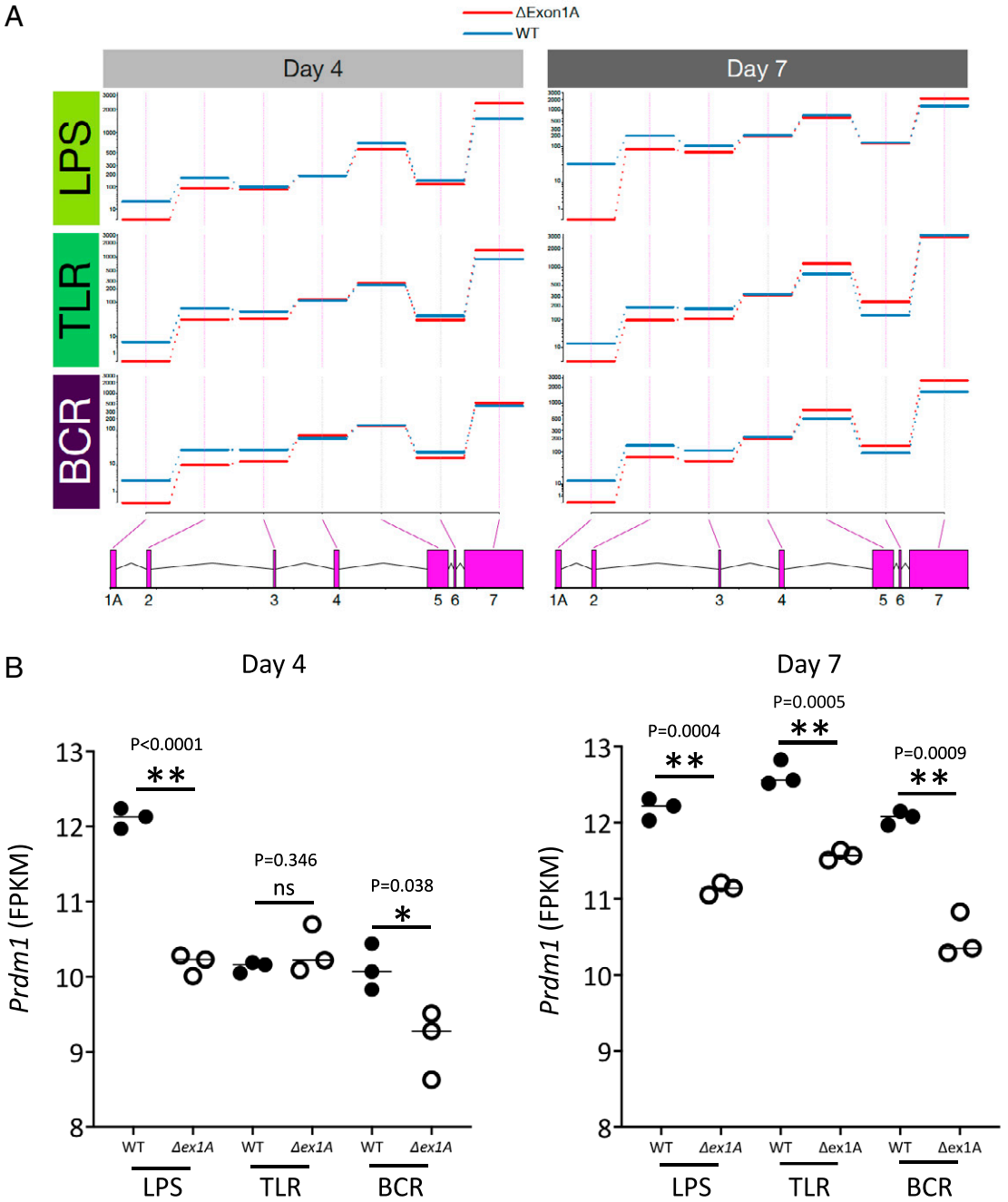

FIGURE 6. TLR and BCR stimulation conditions drive expression of *Prdm1* from multiple promoters. (**A**) Relative exon usage was calculated for each exon (RefSeq annotation) at day 4 or 7 following the indicated culture conditions using three individual mice per condition. Transcripts for WT are shown in blue and Δ*ex1A* in red. (**B**) Relative expression levels of *Prdm1* at day 4 or 7 of the indicated cultures. Results show values from three individual mice with significance determined by unpaired *t* test.

Discussion

We have described a novel system suitable for generating murine plasma cells through either TLR or BCR engagement in conjunction with CD40 ligation and sequential cytokine addition. Validation experiments showed that in vitro generated cells display similar characteristics to in vivo murine plasma cells. For example, phenotypic analysis revealed that downregulation of the pan B cell marker B220 occurred concurrently with upregulation of the plasma cell marker CD138.

Furthermore, the use of a Blimp-1–Venus reporter confirmed the expected upregulation during differentiation, consistent with the use of high Blimp-1 expression to identify plasma cells (14). Unexpectedly

Transcripts originating from exon 1C retain the intervening intron upstream of exon 2. (**B**) Purified B-2 splenic B cells from WT or Δ*ex1A* mice cultured in either LPS, TLR, or BCR conditions were analyzed using flow cytometry on day 4 and 7 for B220 and CD138. Plots are representative of two independent experiments each performed with three mice. (**C**) Cell number was recorded at the indicated time points. Results are displayed as the mean ± SD for 3 individual mice. (**D**) Supernatant was collected at day 4 and 7 from in vitro cultures. IgM and IgG concentrations were quantified using an ELISA and normalized using cell counts and the amount of time in culture. Results are displayed as the mean ± SD for three individual mice.

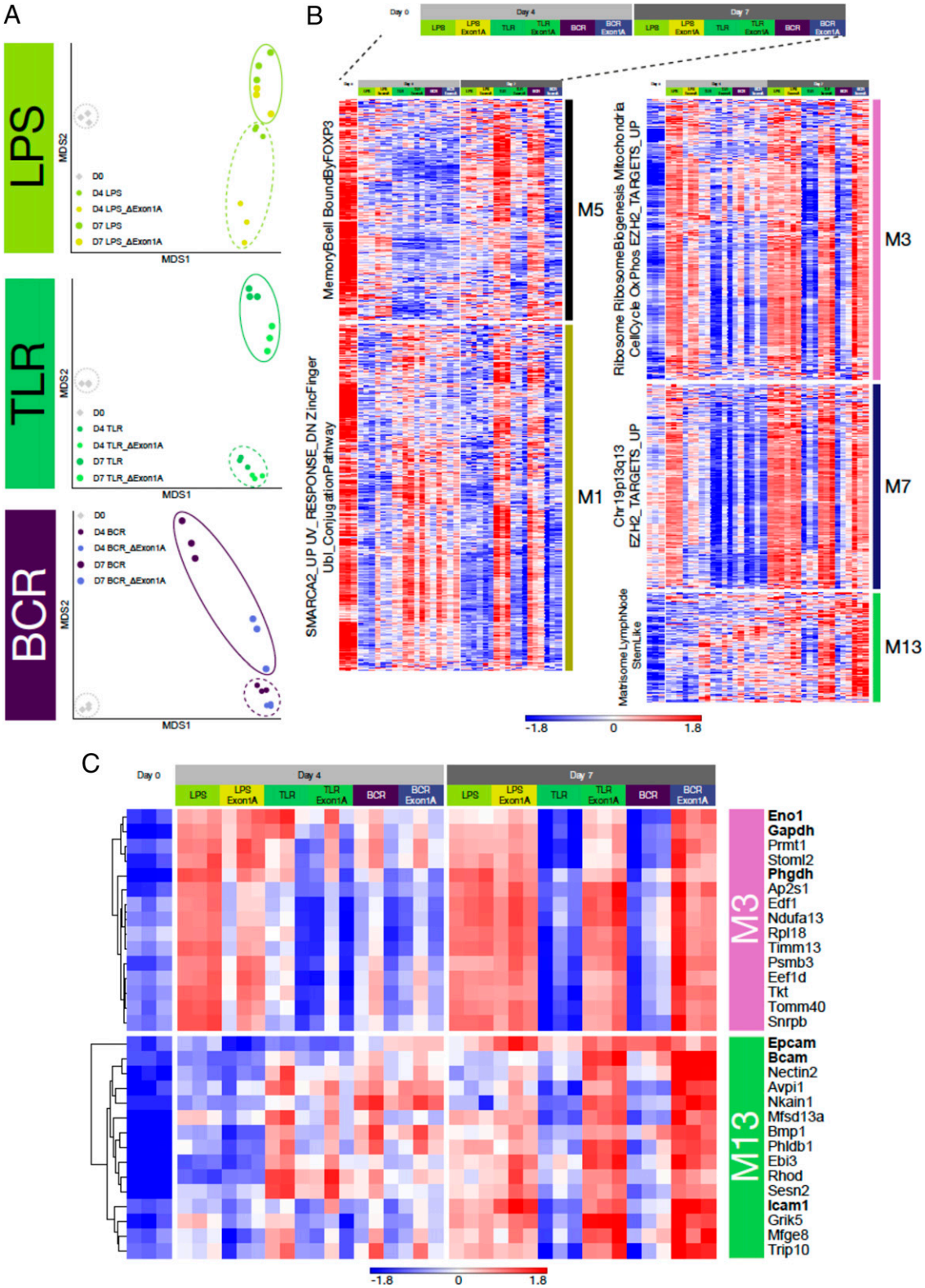

FIGURE 7. Gene expression profiling of cells derived from Δ*ex1A* mice. (**A**) MDS analysis of RNA-seq data from day 4 and 7 cells derived from WT or Δ*ex1A* mice cultured in the indicated conditions. (**B**) Selected module expression values illustrated as heatmap showing the expression across three independent differentiations per time point. In each set, the WT and Δ*ex1A* samples are shown side-by-side and grouped according to stimulation with LPS, TLR, and BCR from left to right. (**C**) Selected gene expression from modules M3 and M13.

between day 9 and 13, Blimp-1 expression as detected by this system, decreased slightly in both TLR and BCR stimulated cells. Blimp-1 functions primarily as a transcriptional repressor, either through competition with activators (33, 34) or recruitment of corepressors such as HDAC1/2 (35), G9A (36), or EZH2 (37). Therefore, it is conceivable that once target loci are silenced there may be a reduction in the level of Blimp-1 required to sustain heterochromatinization.

Both sets of conditions predominantly promoted IgM secretion; however, a proportion of cells were capable of producing class-switched IgG. This could suggest that the cytokines used in these conditions are weak drivers of class switch recombination, however alternative isotypes and IgG subtypes have not yet been investigated. Alternative cytokines have been shown to specifically promote switching to other isotypes, such as TGF-β which promotes IgA (38) and IFN, which promotes IgG2a (39). Although not explicitly tested, the prediction is that inclusion of other cytokines may allow the generation of different types of Ig. However, both TGF-β and IFN have additional effects on B cell proliferation and survival (40, 41) that could alter the plasma cell output in vitro, thus necessitating a careful examination of the impact of any cytokine alterations in the system.

As there is a strong correlation between the concentration of cytokines in culture, the time taken for a cell to divide and the differentiation state of an ASC (42), proliferative capacity of the cells was examined across the differentiation. After assessing proliferation at various time points, results showed that a high division rate accompanied maturation of murine B cells to plasmablasts before cessation of proliferation at roughly day 8, which was verified by the gene expression data. Plasma cells were then able to persist in the absence of any additional division and shown to survive for extended periods of time.

Gene expression analysis confirmed that cells were indeed plasma cell–like when stimulated with either TLR or BCR conditions. The cells obtained at day 10 displayed a common gene program consistent with bone marrow plasma cells described by Shi and colleagues (13). Although the overall gene expression profile appeared to be similar when using either TLR or BCR stimuli, there were striking differences. TLR engagement led to an accelerated and enhanced plasma cell signature, in keeping with previous reports of synergistic enhancement of differentiation when TLR agonists are coupled with a CD40 signal (43, 44). In contrast, BCR conditions promoted a distinct and sustained induction of genes linked to the matrisome, which is composed of ECM-associated proteins, regulators, and secreted factors (45). This pronounced shift in gene expression may allow altered cell adhesion, motility or differential signaling that impact on the ability of plasma cells to integrate within supportive niches for long-term survival.

The utility of the newly described TLR and BCR culture systems is underscored by the results obtained using B cells with a targeted deletion of the *Prdm1* exon 1A promoter region. While investigating the requirement of exon 1A for Blimp-1 expression, it became clear that Δ*ex1A* cells stimulated with LPS were able to differentiate into ASCs. This was also the case for cells differentiated using TLR conditions; however, cells cultured in BCR conditions were unable to upregulate CD138 resulting in a population of $B220^{-}CD138^{-}$ cells. Furthermore, Δ*ex1A* cells cultured in BCR conditions lacked transcripts corresponding to the regulatory region of *Prdm1* and exhibited lower *Prdm1* expression compared with both WT cells and Δ*ex1A* cells cultured in either LPS or TLR conditions. As the two conditions differ in the type of receptor engagement (i.e., BCR crosslinking or TLR4 binding), it is plausible that TLR4 signaling overcomes the loss of exon 1A to maintain *Prdm1* expression. In previous work, Morgan and colleagues established the presence of NF-κB sites upstream of the exon 1A promoter, which were essential for *Prdm1* induction and plasma cell differentiation (15). In agreement with this finding, stimulated B cells isolated from mice lacking RelA, a subunit of NF-κB, in the B cell lineage have a severely reduced number of plasmablasts as well as dramatically impaired induction of Blimp-1 (46). Collectively, this supports the idea that TLR4 signaling may use alternative regulatory regions within *Prdm1* to enable differentiation. In contrast, essential signals required for *Prdm1* activation are lost using the combination of Δ*ex1A* and BCR signaling.

The ability of Δ*ex1A* B cells to generate ASCs in response to LPS is contrary to the results published by Morgan and colleagues (15). However, their evaluation was conducted on total splenocytes stimulated for 3 d and may therefore have failed to detect low levels of Blimp-1 generated at this time point. It is also worth noting that when bone marrow–derived dendritic cells from exon 1A deficient mice were stimulated with LPS, the cells still produced Blimp-1 protein, albeit at a reduced level. The authors identified substantial expression of *Prdm1* transcripts originating from at least one other promoter (exon 1C) in these mice, and therefore the results presented in this study promote the idea that the B cell lineage is potentially capable of using alternative promoters in different contexts, although it remains to be corroborated in vivo.

In conclusion, the validated models presented in this study provide a foundation to systematically explore the terminal stages of murine B cell differentiation, make use of genetic models to probe the role of individual molecules in a cell-autonomous manner and lay the groundwork for confirmatory studies in whole animal models.

Acknowledgments

We thank Elizabeth Bikoff and Elizabeth Robertson for providing mice and the Leeds Institute of Medical Research Flow Cytometry Facility and Next Generation Sequencing Facility for technical support.

Disclosures

The authors have no financial conflicts of interest.

References

1. Renshaw, B. R., W. C. Fanslow III, R. J. Armitage, K. A. Campbell, D. Liggitt, B. Wright, B. L. Davison, and C. R. Maliszewski. 1994. Humoral immune responses in CD40 ligand-deficient mice. *J. Exp. Med.* 180: 1889–1900.
2. Foy, T. M., J. D. Laman, J. A. Ledbetter, A. Aruffo, E. Claassen, and R. J. Noelle. 1994. gp39-CD40 interactions are essential for germinal center formation and the development of B cell memory. *J. Exp. Med.* 180: 157–163.
3. Kawabe, T., T. Naka, K. Yoshida, T. Tanaka, H. Fujiwara, S. Suematsu, N. Yoshida, T. Kishimoto, and H. Kikutani. 1994. The immune responses in CD40-deficient mice: impaired immunoglobulin class switching and germinal center formation. *Immunity* 1: 167–178.
4. Good-Jacobson, K. L., and M. J. Shlomchik. 2010. Plasticity and heterogeneity in the generation of memory B cells and long-lived plasma cells: the influence of germinal center interactions and dynamics. *J. Immunol.* 185: 3117–3125.
5. Roth, K., L. Oehme, S. Zehentmeier, Y. Zhang, R. Niesner, and A. E. Hauser. 2014. Tracking plasma cell differentiation and survival. *Cytometry A* 85: 15–24.
6. Robinson, M. J., R. H. Webster, and D. M. Tarlinton. 2020. How intrinsic and extrinsic regulators of plasma cell survival might intersect for durable humoral immunity. *Immunol. Rev.* 296: 87–103.
7. Jourdan, M., A. Caraux, J. De Vos, G. Fiol, M. Larroque, C. Cognot, C. Bret, C. Duperray, D. Hose, and B. Klein. 2009. An in vitro model of differentiation of memory B cells into plasmablasts and plasma cells including detailed phenotypic and molecular characterization. *Blood* 114: 5173–5181.
8. Jourdan, M., M. Cren, N. Robert, K. Bolloré, T. Fest, C. Duperray, F. Guilloton, D. Hose, K. Tarte, and B. Klein. 2014. IL-6 supports the generation of human long-lived plasma cells in combination with either APRIL or stromal cell-soluble factors. *Leukemia* 28: 1647–1656.
9. Cocco, M., S. Stephenson, M. A. Care, D. Newton, N. A. Barnes, A. Davison, A. Rawstron, D. R. Westhead, G. M. Doody, and R. M. Tooze. 2012. In vitro generation of long-lived human plasma cells. *J. Immunol.* 189: 5773–5785.
10. Nguyen, D. C., S. Garimalla, H. Xiao, S. Kyu, I. Albizua, J. Galipeau, K. Y. Chiang, E. K. Waller, R. Wu, G. Gibson, et al. 2018. Factors of the bone marrow microniche that support human plasma cell survival and immunoglobulin secretion. [Published erratum appears in 2019 *Nat. Commun.* 10: 372.] *Nat. Commun.* 9: 3698.
11. Nutt, S. L., P. D. Hodgkin, D. M. Tarlinton, and L. M. Corcoran. 2015. The generation of antibody-secreting plasma cells. *Nat. Rev. Immunol.* 15: 160–171.
12. Hasbold, J., L. M. Corcoran, D. M. Tarlinton, S. G. Tangye, and P. D. Hodgkin. 2004. Evidence from the generation of immunoglobulin G-secreting cells that stochastic mechanisms regulate lymphocyte differentiation. *Nat. Immunol.* 5: 55–63.
13. Shi, W., Y. Liao, S. N. Willis, N. Taubenheim, M. Inouye, D. M. Tarlinton, G. K. Smyth, P. D. Hodgkin, S. L. Nutt, and L. M. Corcoran. 2015. Transcriptional profiling of mouse B cell terminal differentiation defines a signature for antibody-secreting plasma cells. *Nat. Immunol.* 16: 663–673.
14. Tellier, J., W. Shi, M. Minnich, Y. Liao, S. Crawford, G. K. Smyth, A. Kallies, M. Busslinger, and S. L. Nutt. 2016. Blimp-1 controls plasma cell function

through the regulation of immunoglobulin secretion and the unfolded protein response. *Nat. Immunol.* 17: 323–330.
15. Morgan, M. A., E. Magnusdottir, T. C. Kuo, C. Tunyaplin, J. Harper, S. J. Arnold, K. Calame, E. J. Robertson, and E. K. Bikoff. 2009. Blimp-1/Prdm1 alternative promoter usage during mouse development and plasma cell differentiation. *Mol. Cell. Biol.* 29: 5813–5827.
16. Scharer, C. D., B. G. Barwick, M. Guo, A. P. R. Bally, and J. M. Boss. 2018. Plasma cell differentiation is controlled by multiple cell division-coupled epigenetic programs. *Nat. Commun.* 9: 1698.
17. Ozcan, E., L. Garibyan, J. J. Lee, R. J. Bram, K. P. Lam, and R. S. Geha. 2009. Transmembrane activator, calcium modulator, and cyclophilin ligand interactor drives plasma cell differentiation in LPS-activated B cells. *J. Allergy Clin. Immunol.* 123: 1277–86.e5.
18. Ohinata, Y., M. Sano, M. Shigeta, K. Yamanaka, and M. Saitou. 2008. A comprehensive, non-invasive visualization of primordial germ cell development in mice by the Prdm1-mVenus and Dppa3-ECFP double transgenic reporter. *Reproduction* 136: 503–514.
19. Dobin, A., C. A. Davis, F. Schlesinger, J. Drenkow, C. Zaleski, S. Jha, P. Batut, M. Chaisson, and T. R. Gingeras. 2013. STAR: ultrafast universal RNA-seq aligner. *Bioinformatics* 29: 15–21.
20. Li, B., and C. N. Dewey. 2011. RSEM: accurate transcript quantification from RNA-Seq data with or without a reference genome. *BMC Bioinformatics* 12: 323.
21. Soneson, C., M. I. Love, and M. D. Robinson. 2015. Differential analyses for RNA-seq: transcript-level estimates improve gene-level inferences. *F1000 Res.* 4: 1521.
22. Love, M. I., W. Huber, and S. Anders. 2014. Moderated estimation of fold change and dispersion for RNA-seq data with DESeq2. *Genome Biol.* 15: 550.
23. Zhu, A., J. G. Ibrahim, and M. I. Love. 2019. Heavy-tailed prior distributions for sequence count data: removing the noise and preserving large differences. *Bioinformatics* 35: 2084–2092.
24. Johnson, W. E., C. Li, and A. Rabinovic. 2007. Adjusting batch effects in microarray expression data using empirical Bayes methods. *Biostatistics* 8: 118–127.
25. Care, M. A., D. R. Westhead, and R. M. Tooze. 2019. Parsimonious Gene Correlation Network Analysis (PGCNA): a tool to define modular gene co-expression for refined molecular stratification in cancer. *NPJ Syst. Biol. Appl.* 5: 13.
26. Anders, S., A. Reyes, and W. Huber. 2012. Detecting differential usage of exons from RNA-seq data. *Genome Res.* 22: 2008–2017.
27. Steinman, R. M., S. J. Blumencranz, B. G. Machtinger, J. Fried, and Z. A. Cohn. 1978. Mouse spleen lymphoblasts generated in vitro. Their replication and differentiation in vitro. *J. Exp. Med.* 147: 297–315.
28. Shapiro-Shelef, M., K. I. Lin, L. J. McHeyzer-Williams, J. Liao, M. G. McHeyzer-Williams, and K. Calame. 2003. Blimp-1 is required for the formation of immunoglobulin secreting plasma cells and pre-plasma memory B cells. *Immunity* 19: 607–620.
29. Oracki, S. A., J. A. Walker, M. L. Hibbs, L. M. Corcoran, and D. M. Tarlinton. 2010. Plasma cell development and survival. *Immunol. Rev.* 237: 140–159.
30. Tunyaplin, C., M. A. Shapiro, and K. L. Calame. 2000. Characterization of the B lymphocyte-induced maturation protein-1 (Blimp-1) gene, mRNA isoforms and basal promoter. *Nucleic Acids Res.* 28: 4846–4855.
31. Morgan, M. A., A. W. Mould, L. Li, E. J. Robertson, and E. K. Bikoff. 2012. Alternative splicing regulates Prdm1/Blimp-1 DNA binding activities and corepressor interactions. *Mol. Cell. Biol.* 32: 3403–3413.
32. Smith, M. A., M. Maurin, H. I. Cho, B. Becknell, A. G. Freud, J. Yu, S. Wei, J. Djeu, E. Celis, M. A. Caligiuri, and K. L. Wright. 2010. PRDM1/Blimp-1 controls effector cytokine production in human NK cells. *J. Immunol.* 185: 6058–6067.
33. Kuo, T. C., and K. L. Calame. 2004. B lymphocyte-induced maturation protein (Blimp)-1, IFN regulatory factor (IRF)-1, and IRF-2 can bind to the same regulatory sites. *J. Immunol.* 173: 5556–5563.
34. Tooze, R. M., S. Stephenson, and G. M. Doody. 2006. Repression of IFN-gamma induction of class II transactivator: a role for PRDM1/Blimp-1 in regulation of cytokine signaling. *J. Immunol.* 177: 4584–4593.
35. Yu, J., C. Angelin-Duclos, J. Greenwood, J. Liao, and K. Calame. 2000. Transcriptional repression by blimp-1 (PRDI-BF1) involves recruitment of histone deacetylase. *Mol. Cell. Biol.* 20: 2592–2603.
36. Gyory, I., J. Wu, G. Fejér, E. Seto, and K. L. Wright. 2004. PRDI-BF1 recruits the histone H3 methyltransferase G9a in transcriptional silencing. *Nat. Immunol.* 5: 299–308.
37. Minnich, M., H. Tagoh, P. Bönelt, E. Axelsson, M. Fischer, B. Cebolla, A. Tarakhovsky, S. L. Nutt, M. Jaritz, and M. Busslinger. 2016. Multifunctional role of the transcription factor Blimp-1 in coordinating plasma cell differentiation. *Nat. Immunol.* 17: 331–343.
38. Ehrhardt, R. O., W. Strober, and G. R. Harriman. 1992. Effect of transforming growth factor (TGF)-beta 1 on IgA isotype expression. TGF-beta 1 induces a small increase in sIgA+ B cells regardless of the method of B cell activation. *J. Immunol.* 148: 3830–3836.
39. Bossie, A., and E. S. Vitetta. 1991. IFN-gamma enhances secretion of IgG2a from IgG2a-committed LPS-stimulated murine B cells: implications for the role of IFN-gamma in class switching. *Cell. Immunol.* 135: 95–104.
40. Kehrl, J. H., A. B. Roberts, L. M. Wakefield, S. Jakowlew, M. B. Sporn, and A. S. Fauci. 1986. Transforming growth factor beta is an important immunomodulatory protein for human B lymphocytes. *J. Immunol.* 137: 3855–3860.
41. Hasbold, J., J. S. Hong, M. R. Kehry, and P. D. Hodgkin. 1999. Integrating signals from IFN-gamma and IL-4 by B cells: positive and negative effects on CD40 ligand-induced proliferation, survival, and division-linked isotype switching to IgG1, IgE, and IgG2a. *J. Immunol.* 163: 4175–4181.
42. Zhou, J. H. S., J. F. Markham, K. R. Duffy, and P. D. Hodgkin. 2018. Stochastically timed competition between division and differentiation fates regulates the transition from B lymphoblast to plasma cell. *Front. Immunol.* 9: 2053.
43. Knödel, M., A. W. Kuss, I. Berberich, and A. Schimpl. 2001. Blimp-1 overexpression abrogates IL-4- and CD40-mediated suppression of terminal B cell differentiation but arrests isotype switching. *Eur. J. Immunol.* 31: 1972–1980.
44. Pone, E. J., Z. Lou, T. Lam, M. L. Greenberg, R. Wang, Z. Xu, and P. Casali. 2015. B cell TLR1/2, TLR4, TLR7 and TLR9 interact in induction of class switch DNA recombination: modulation by BCR and CD40, and relevance to T-independent antibody responses. *Autoimmunity* 48: 1–12.
45. Hynes, R. O., and A. Naba. 2012. Overview of the matrisome–an inventory of extracellular matrix constituents and functions. *Cold Spring Harb. Perspect. Biol.* 4: a004903.
46. Heise, N., N. S. De Silva, K. Silva, A. Carette, G. Simonetti, M. Pasparakis, and U. Klein. 2014. Germinal center B cell maintenance and differentiation are controlled by distinct NF-κB transcription factor subunits. *J. Exp. Med.* 211: 2103–2118.